

## MIT Open Access Articles

*A multilayered microfluidic blood vessel-like structure*

The MIT Faculty has made this article openly available. **Please share** how this access benefits you. Your story matters.

**Citation:** Hasan, Anwarul et al. "A Multilayered Microfluidic Blood Vessel-like Structure." Biomedical Microdevices 17.5 (2015): n. pag.

**As Published:** <http://dx.doi.org/10.1007/s10544-015-9993-2>

**Publisher:** Springer US

**Persistent URL:** <http://hdl.handle.net/1721.1/103996>

**Version:** Author's final manuscript: final author's manuscript post peer review, without publisher's formatting or copy editing

**Terms of Use:** Article is made available in accordance with the publisher's policy and may be subject to US copyright law. Please refer to the publisher's site for terms of use.



# A multilayered microfluidic blood vessel-like structure

Anwarul Hasan<sup>1,2,3</sup> · Arghya Paul<sup>2,3,4,5</sup> · Adnan Memic<sup>6</sup> · Ali Khademhosseini<sup>2,3,5,7,8</sup>

Published online: 11 August 2015  
© Springer Science+Business Media New York 2015

**Abstract** There is an immense need for tissue engineered blood vessels. However, current tissue engineering approaches still lack the ability to build native blood vessel-like perfusable structures with multi-layered vascular walls. This paper demonstrated a new method to fabricate tri-layer biomimetic blood vessel-like structures on a microfluidic platform using photocrosslinkable gelatin hydrogel. The presented method enables fabrication of physiological blood vessel-like structures with mono-, bi- or tri-layer vascular walls. The diameter of the vessels, the total thickness of the vessel wall and the thickness of each individual layer of the wall were independently controlled. The developed fabrication process is a simple and rapid method, allowing the physical fabrication of the vascular structure in minutes, and the formation of a vascular endothelial cell layer inside the vessels in 3–5 days. The fabricated vascular constructs can potentially be used in numerous applications including drug screening, development of *in vitro* models for

cardiovascular diseases and/or cancer metastasis, and study of vascular biology and mechanobiology.

**Keywords** Tissue engineering · Microfluidics · Blood vessel · Hydrogel · PDMS · Microfabrication

## 1 Introduction

Cardiovascular diseases are amongst the major causes of fatalities worldwide (Hasan et al. 2015; Tu et al. 1997; Ratcliffe 2000). Each year 1.4 million patients in US alone need arterial prosthesis (Browning et al. 2012). This has created a tremendous need for tissue engineered artificial blood vessels that could be used not only for replacement or bypass of damaged arteries but also for the development of *in vitro* models of vascular diseases, drug discovery and organ-on-a-chip plat-

---

**Electronic supplementary material** The online version of this article (doi:10.1007/s10544-015-9993-2) contains supplementary material, which is available to authorized users.

---

✉ Anwarul Hasan  
mh211@aub.edu.lb

✉ Ali Khademhosseini  
alik@rics.bwh.harvard.edu

<sup>1</sup> Biomedical Engineering, and Department of Mechanical Engineering, Faculty of Engineering and Architecture, American University of Beirut, Beirut 1107 2020, Lebanon

<sup>2</sup> Biomaterials Innovation Research Center, Division of Biomedical Engineering, Department of Medicine, Brigham and Women's Hospital, Harvard Medical School, Cambridge, MA 02139, USA

<sup>3</sup> Harvard-MIT Division of Health Sciences and Technology, Massachusetts Institute of Technology, Cambridge, MA 02139, USA

<sup>4</sup> Department of Chemical and Petroleum Engineering, University of Kansas, Lawrence, KS 66045-7609, USA

<sup>5</sup> Wyss Institute for Biologically Inspired Engineering, Harvard University, Boston, MA 02115, USA

<sup>6</sup> Center of Nanotechnology, King Abdulaziz University, Jeddah 21589, Saudi Arabia

<sup>7</sup> World Premier International – Advanced Institute for Materials Research (WPI-AIMR), Tohoku University, Sendai 980-8577, Japan

<sup>8</sup> Department of Physics, King Abdulaziz University, Jeddah 21589, Saudi Arabia

forms (Hasan et al. 2014a, b). Besides, for widespread clinical application of tissue engineering, vascularization of three dimensional (3D) tissue constructs remains a major problem (Barthes et al. 2014; Du et al. 2008; Hasan et al. 2014d; Miller et al. 2012; Novosel et al. 2011; Sudo et al. 2009). The development of proper vascularization methods will enable tissue engineering of thick, complex 3D tissue constructs, particularly those comprising large vital organs such as liver, kidney and heart (Kaully et al. 2009). Similarly, the ability to form artificial blood vessels on-chip will pave the way for development of *in vitro* models of vascular diseases, which could revolutionize the generation of new therapeutics for atherosclerosis, hypertension, heart attack, stroke and many other diseases (Hasan et al. 2014a, b). Extensive research over the past two decades has been aimed at the development of viable tissue engineered blood vessels. However, achieving the goal of a viable tissue engineered blood vessel remains elusive. In particular, the current approaches of tissue engineering still lack the ability to form perfusable blood vessels with native-like tri-layered architecture.

Researchers have employed numerous methods to form blood vessel-like structures *in vitro* which can be broadly classified into two types, namely (i) angiogenesis based approaches forming blood vessel capillaries and (ii) prevascularization based approaches for generating larger vessels. In the angiogenesis based approaches, the directional migration and self-organization of specific cell types under controlled microenvironments are used for promoting the formation of microvascular-like structures (Chung et al. 2009; Sudo et al. 2009; Saik et al. 2012; Leslie-Barbick et al. 2009, 2011a, b; Chen et al. 2007; Cao et al. 2009; Yuen et al. 2010; Yeon et al. 2012; Mendes et al. 2012; Chen et al., 2012). For instance, a sprouting assay of endothelial cells (ECs) on microbeads was introduced where vascular tube-like structures were successfully formed (Shamloo and Heilshorn 2010; Shamloo et al. 2012; Nakatsu et al. 2003). However, these vascular structures were closed. Kamm and colleagues used co-culture of ECs with fibroblast cells in a microfluidic-based approach to guide a directional migration of EC into a hydrogel, resulting in formation of endothelial sprouts and hence blood vessel capillary-like structures (Chung et al. 2009; Sudo et al. 2009). West (Saik et al. 2012; Leslie-Barbick et al. 2009, 2011a, b) and Mooney (Chen et al. 2007; Cao et al. 2009; Yuen et al. 2010) used immobilization and delivery of various angiogenic growth factors in matrix materials for promoting formation of vascular structures. Co-culture of various cells such as ECs with mesenchymal stem cells (MSCs) in type I collagen or Matrigel (Darland and D'Amore 2001) and endothelial colony forming cells (ECFCs) with MSCs in gelatin methacryloyl (GelMA) (Chen et al. 2012) were also investigated. However, limitations of these approaches include the fact that the structures formed using these approaches are not readily perfusable.

In the alternative prevascularization based approaches, vascular structures are formed by encapsulating or surface seeding vascular cells in a preformed vascular network or tube within a 3D hydrogel construct. A major advantage of this approach is that it allows immediate perfusion of the constructs, helping the growth and proliferation of the cells. Moreover, the delivery of oxygen and nutrients, and the removal of metabolic wastes can be performed continuously (Price et al. 2010; Chrobak et al. 2006; Zheng et al. 2012; Sadr et al. 2011; Miller et al. 2012; Yoshida et al. 2012; Khademhosseini et al. 2004, 2005). However, vascular constructs reported so far based on this approach consisted of either a single monolayer of ECs (Price et al. 2010; Chrobak et al. 2006), or a bilayered construct of ECs with smooth muscle cells (SMCs) in one example (Yoshida et al. 2012). The native arterial and venous wall on the other hand are composed of three layers: (i) tunica intima, a continuous monolayer of ECs, (ii) tunica media, dense populations of concentrically organized SMCs, and (iii) adventitia, a collagenous extracellular matrix (ECM) that mainly contains fibroblast cells and perivascular nerve cells. Fully recapitulating the well-organized tri-layer wall structure is important for proper functioning of artificial tissue engineered blood vessels. A tri-layer structure could also provide better understanding of the cell-cell signaling and interactions between the ECs, SMCs, and fibroblast cells during the initiation, progression and curing of various vascular diseases.

Here we report the development of a tri-layered perfusable vascular-like structure on a microfluidic platform using a simple method based on a concentric layer-by-layer organization of vascular cells, namely, fibroblast cells, SMCs and ECs in a photocrosslinkable 3D hydrogel. We choose GelMA hydrogels because of their tunable mechanical properties and the fast and easy crosslinking with precise control over the time and density of photocrosslinking. The tri-layer structures of 0.6 and 1.2 mm outer diameters can be formed with lumen diameters in the range of 120–400  $\mu\text{m}$  and the lumen to wall thickness ratio of 0.22–1.0. The mechanical properties of the walls of the vascular-like structures can also be varied by varying the GelMA concentration in the range 4–16 %. The higher concentration GelMA (12 % and higher) resulted in better vessel structures with smoother luminal surfaces compared to lower concentration GelMA. A confluent monolayer of EC in the luminal surface was formed in 3–5 days and barrier function of the endothelial monolayer was analyzed in detail using the permeation of fluorescently labeled probes. The vessels demonstrated here could be useful in numerous applications including development of *in vitro* human tissue based platforms for drug discovery, disease models and mechano-biological studies.

## 2 Experimental

### 2.1 Materials and reagents

Polydimethylsiloxane (PDMS; Sylgard 184) was purchased from Dow Corning, Midland, MI). Petri dishes, cover slips, and glass slides were purchased from Fisher Scientific (Philadelphia, USA). Type A gelatin (porcine skin), 3-(trimethoxysilyl)propyl methacrylate (TMSPMA), and methacrylic anhydride (MA), were obtained from Sigma-Aldrich (Wisconsin, USA). Irgacure 2959 photoinitiator (2-hydroxy-1-(4-(hydroxyethoxy), phenyl)-2-methyl-1-propanone purchased from CIBA Chemicals) was initiated by an ultraviolet (UV) light source (Omnigore S2000) manufactured by EXFO Photonic Solutions Inc. (Canada). 120  $\mu\text{m}$ , 200  $\mu\text{m}$  and 300  $\mu\text{m}$ -diameter; 30 and 40 mm long stainless steel acupuncture needles were purchased from Seirin Corporation, Japan, while 400  $\mu\text{m}$ , 500  $\mu\text{m}$  and 800  $\mu\text{m}$  hypodermic stainless steel needles (27G, and 21G respectively) were purchased from BD precisionGlide<sup>®</sup>, Franklin Lakes, NJ. Endothelial basal medium-2 (EBM-2, CC-3156, Lonza) and endothelial growth bulletkit (EGM-2; CC-3162, Lonza) supplements were purchased from Lonza (Switzerland). All other chemicals and reagents were purchased from Sigma Aldrich (USA) unless otherwise indicated.

### 2.2 GelMA synthesis

Synthesis of GelMA was performed as described previously (Van Den Bulcke et al. 2000; Nichol et al. 2010; Benton et al. 2009; Paul et al. 2014). In brief, type-A gelatin obtained from porcine skin was dissolved in Dulbecco's phosphate buffered saline (DPBS) (Gibco, USA), at 10 % (*w/v*) concentration by heating at 60 °C on a hot plate while continuously stirring for 1 h using a magnetic stirrer. Then, 8 ml of methacrylic anhydride was added drop-wise per 100 ml of gelatin solution at a rate of 0.5 ml/min, keeping the temperature at 50 °C and continuously stirring the solution for 3 h. The solution was then diluted to 1/5th of the initial concentration by adding pre-warmed (40 °C) DPBS, thereby stopping any further reaction. The diluted mixture was dialyzed using a 12–14 kDa dialysis membrane for 1 week against distilled water at 40 °C, followed by filtration through a 0.2  $\mu\text{m}$  filter, overnight storage at –80 °C, and finally, lyophilizing for 1 week. This white porous foam of GelMA was stored at –80 °C until further use.

### 2.3 Cell culture

The cells used in this study were of three different types, namely, (i) human umbilical vein endothelial cells (HUVECs;

a generous gift from Dr. J. Folkman, Children's Hospital, Boston) with constitutive green fluorescent protein (GFP) expression, (ii) rat aortic SMCs, and (iii) 3T3 fibroblast cells. The cell culture media for HUVECs was prepared using endothelial growth bulletkit (EGM-2; Lonza) supplement in endothelial basal medium, (EBM-2; Lonza), with 10 % fetal bovine serum (FBS) and 1 % penicillin plus streptomycin. The SMC and 3T3 media consisted of Dulbecco's Modified Eagle Medium, DMEM, supplemented with 10 % FBS and 1 % penicillin plus streptomycin. The cells were cultured at 37 °C, in standard cell culture incubator (5 % CO<sub>2</sub>) for up to 70–80 % confluence before passaging to new flasks or using them in an experiment.

### 2.4 Fabrication of PDMS microfluidic device

The microfluidic device was fabricated using small glass capillary tubes (1.2 and 0.6 mm internal diameter, 15 mm long) embedded in a PDMS device to provide it with mechanical support and stability. The device consisted of three layers: (i) the top layer, a rectangular PDMS slab with an inlet and outlet tubing connected to it, (ii) the middle layer containing two punched holes for inlet and outlet reservoirs and a channel to house the vessel to be fabricated, and (iii) the bottom layer, a rectangular piece of glass slide. At first the inner surface of the glass capillaries/tubes were coated with TMSPMA coating (Nichol et al. 2010). The glass capillaries of desired size were immobilized in a petri dish using PDMS glue. The capillaries were then casted in PDMS rubber by pouring liquid PDMS (10:1 ratio of silicon base Sylgard to curing agent) in the petri dish. The liquid PDMS was cured at 80 °C in an oven for 2 h upon which it became solidified. The flat PDMS, was cut into rectangular parts (15 × 25 mm), each one with an embedded glass capillary inside. The glass capillary was removed leaving a tubular channel. Two circular holes were punched into the PDMS near the two ends of the capillary channel to make inlet/outlet media reservoirs, and a second piece of glass capillary coated with TMSPMA on their inner surface was inserted inside the channel to replace the first one. This PDMS part was then bonded to the bottom layer of the device using oxygen plasma bonder. The entire device was affixed in a petri dish using PDMS as glue. In an alternate approach, the middle layer of the PDMS device was fabricated by casting liquid PDMS on a silicon wafer mold prepared using microfabrication techniques, and the glass capillary was inserted into the PDMS layer afterwards. The top part of the PDMS device was prepared along with its inlet and outlet tubing to close the PDMS device from top side after the blood vessel fabrication was done. At this stage the microfluidic device was ready for use as shown schematically in Fig. 1a (i).

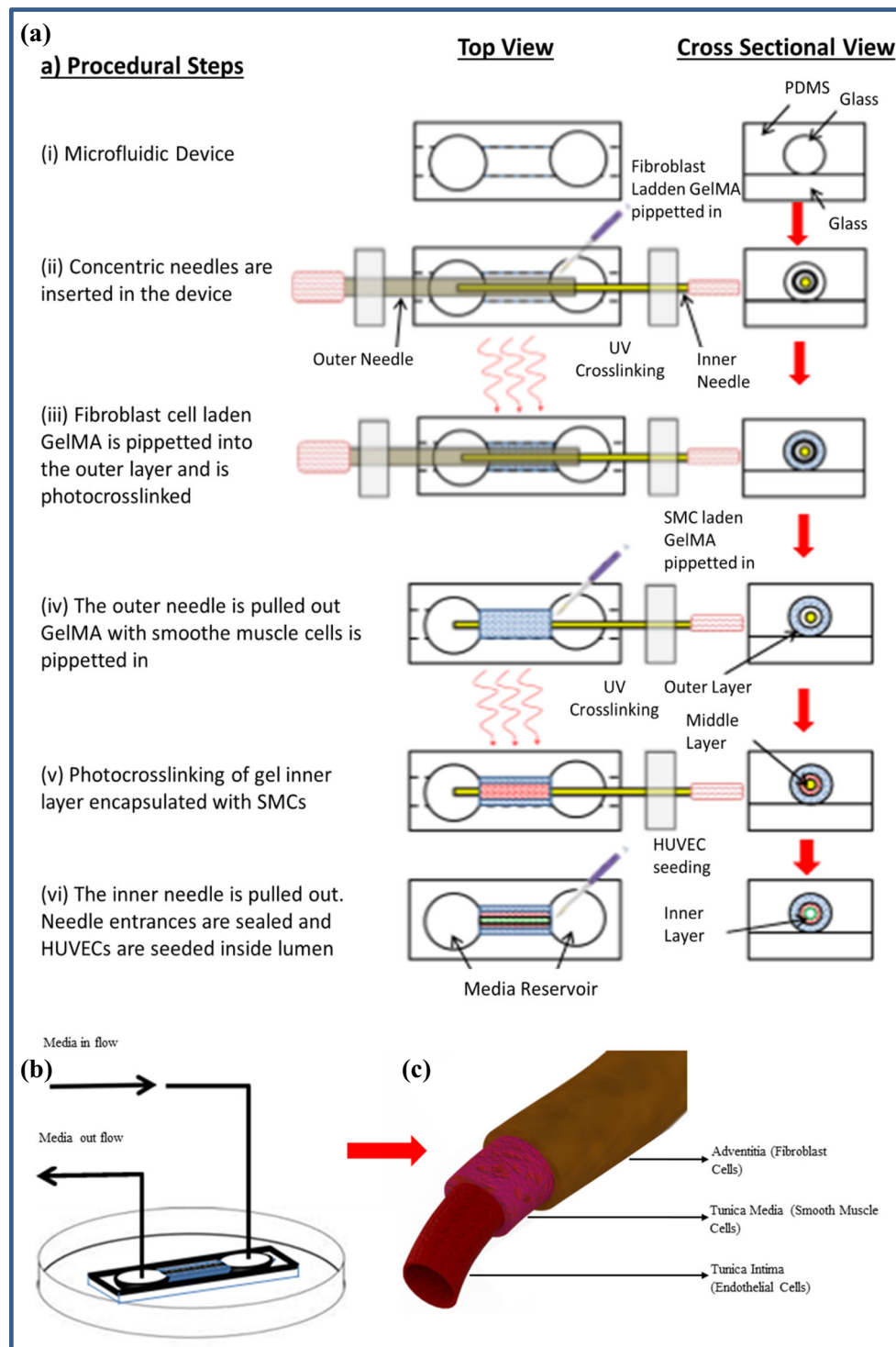


**Fig. 1** Schematic illustration of the step-by-step fabrication process of the tri-layer blood vessel-like structure in a microfluidic device, **a** (i) the middle layer of the three-layer PDMS device was fabricated by casting liquid PDMS on a silicon wafer mold prepared using microfabrication technique or as described in section 2.4. A glass capillary tube was affixed in the channel inside the middle part of the device which was plasma bonded to the bottom layer, a glass slide, (ii) two concentric needles were inserted in the device from opposite ends. The outer space was filled with fibroblast cell-laden GelMA, (iii) the gel outer layer encapsulated with fibroblast cells was photocrosslinked, (iv) The outer

needle was pulled out leaving a concentric annular gap between inner needle and the outer gel layer. GelMA prepolymer solution laden with SMCs was pipetted into the concentric annular space. (v) The inner gel layer, GelMA laden with SMCs, was photocrosslinked. (vi) The inner needle was carefully pulled out leaving a bilayer cellular structure in the microfluidic device. Needle entrances were sealed, and HUVECs were seeded inside lumen resulting in a tri-layer vascular-like structure. **b** Perfusion of cell culture media through the fabricated structure in the microfluidic device was established, **c** the tri-layer vascular structure fabricated through the process



## 2.5 Fabrication of blood vessel-like structures with multilayered vessel walls using concentric needles in GelMA hydrogel

The method that we employed for fabrication of blood vessel-like structures uses a pair of concentric stainless steel needles. The outer needle is a hypodermic needle with its inner diameter being larger than the outer diameter of the inner needle. For fabrication of vessels with different wall thicknesses, different sizes of needle pairs were used, for example 21G, BD (outer diameter: 800  $\mu\text{m}$ , inner diameter: 500  $\mu\text{m}$ ) and 27G, BD (outer diameter: 400  $\mu\text{m}$ , inner diameter: 196  $\mu\text{m}$ ), or 25G, BD (outer diameter: 500  $\mu\text{m}$ , inner diameter: 400  $\mu\text{m}$ ) and 200S Serine needle (outer diameter: 200  $\mu\text{m}$ ) were used respectively.

A schematic representation of the step by step process for fabrication of multilayered vascular structure is presented in Fig. 1a. At first two sterile stainless steel needles were inserted concentrically in the microfluidic device from the two opposite ends, Fig. 1 (ii). Fibroblasts and SMCs were trypsinized from a cell culture flask and mixed in separate GelMA pre-polymer solutions at a density of  $2 \times 10^6$  cells/ml. Different pre-polymer concentrations of GelMA solution were used ranging from 4 to 16 %. The fibroblast cell laden GelMA pre-polymer solution was pipetted into the annular gap between the larger needle and the glass capillary inside the microfluidic device, Fig. 1 (ii), and was crosslinked with light (360–480 nm) at power 5.9  $\text{mw}/\text{cm}^2$ , from a vertical distance of 81 mm by exposing the device to light for 30 s from both top and bottom side, Fig. 1 (iii). The outer needle was pulled out gently leaving a concentric annular gap between the newly formed hydrogel layer and the inner needle. The second pre-polymer GelMA solution, laden with SMC, was pipetted into the concentric annular gap, Fig. 1 (iv), followed by a second-step photocrosslinking, Fig. 1 (v). Finally the inner needle was also gently pulled out creating a bilayer tubular structure with a lumen inside. The needle entrances on both ends of the microfluidic device were sealed using partially cured PDMS. The lumen of the bilayer structure was washed out by flowing PBS through it. In order to pre-condition the bi-layer GelMA construct for seeding of HUVECs, cell culture media was passed through the lumen of the vessel for few hours. HUVECs were trypsinized, centrifuged and suspended in HUVEC media at a cell density of  $20 \times 10^6$  cells/ml. The HUVEC suspension was injected into the lumen of the vessel, observed under the microscope for proper cell loading, and incubated inside the tissue culture incubator for 4 h for cell adhesion to the luminal surface. After 4 h, the non-adherent cells were washed out. The top layer PDMS slab with an inlet and an outlet tubing was connected from the top side of the microfluidic device thereby closing the device. A continuous flow of HUVEC media was set up through the device at a rate of 30–50  $\mu\text{L}/\text{h}$  using a syringe pump. In 3–5 days a fully confluent monolayer of HUVECs was formed on the inner

surface of the lumen, resulting in a tri-layer blood vessel-like structure with fibroblast cells in the outer layer, SMCs in the middle layer and HUVEC mono layer on the luminal surface.

## 2.6 Live-dead staining for cell viability in vessel wall

The viability of 3T3 fibroblast cells in the walls of the vessel was investigated using an Invitrogen live-dead assay kit following supplier protocols. To do so, the media from the well plates was removed and the vessels were washed by PBS. A solution of 2  $\mu\text{L}/\text{ml}$  ethidium homodimer (EthD-1) and 0.5  $\mu\text{L}/\text{ml}$  calcein AM in PBS was added to the well plates, which was then incubated for 20 min inside the incubator at 37  $^\circ\text{C}$ . Finally, the vessels were washed by PBS and the live (green) and dead (red) cells were imaged using an inverted fluorescent microscope (Nikon TE 2000-U, Nikon Instrument Inc., USA). The obtained live-dead staining images were analyzed using the image analysis software ImageJ, whereby the viability of cells was calculated from the ratio of live to total cells.

## 2.7 Phalloidin-DAPI staining for cytoskeletal actin fibers and nuclei of cells

The cells in the vascular structure inside the microfluidic device were fixed on the fifth day after a continuous monolayer of HUVECs was formed on the luminal surface. The cells were fixed in 4 % paraformaldehyde for 30 min, and permeabilized using 0.1 % Triton X for 20 min. 1 % bovine serum albumin (BSA) in PBS was used to block non-specific sites for 1 h. Finally, the cytoskeletal actin fibers of the HUVEC monolayer were stained using Alexa Fluor 488 (green) and the nucleus of the cells were stained with DAPI (blue).

## 2.8 Imaging cross-sections of the engineered vessels

For fluorescent images, the vascular-like structure was fabricated following the same protocol as described in section 2.5 but using fluorescent red, blue and green microbeads instead of the fibroblasts, SMCs and HUVECs. The constructs were then embedded in polyethylene glycol (PEG) hydrogel and sliced into thin layers. For embedding into PEG, 20 % PEG ( $M_w=1000$ ) was dissolved in 0.5 % Irgacure photoinitiator solution prepared using PBS. The pre-polymer solution was pipetted into the lumen of the engineered vascular construct, and was exposed to UV light for 1 min at 5.9  $\text{mw}/\text{cm}^2$  from both top and bottom sides thereby filling the PEG hydrogel inside the lumen. Filling the lumen of the vascular constructs with PEG before sectioning helped in maintaining the circular shape of the cross-sections. The constructs were taken out from the glass capillaries and hence the microfluidic devices by carefully pushing them from one end using a glass rod < 1 mm diameter. For ease of removal of the vessel from the glass capillary

Poly(N-isopropylacrylamide) (polyNipam) coating was applied on them prior to insertion into the microfluidic device. The constructs were then sliced into very thin sections and imaged using fluorescent microscope.

## 2.9 Measurement of mechanical properties

Since the high aspect ratio (long narrow) vessels of hydrogel, as prepared in this study, are susceptible to buckling during axial compressive loading, for stability of the samples during mechanical testing, the cross-section of the vascular constructs was scaled up by five times its original cross-section. To do so, monolayered vascular constructs were formed using  $2 \times 10^6$  cells/ml of SMC encapsulated in GelMA with a 6 mm outer diameter (glass capillary) and 1 mm lumen diameter by using an 18G hypodermic needle in a PDMS device. The vascular constructs after removal from the PDMS device were washed in PBS, cut to 3 mm length, submerged in cell culture media, and stored in the incubator at 37 °C. The constructs were blotted with a KimWipe lightly before placing on the platen for mechanical testing. The uniaxial compressive mechanical tests were performed at a rate of 1 mm/min using an Instron 5943 mechanical tester.

## 2.10 Evaluation of the barrier function of the engineered vessels

To evaluate the barrier function of the HUVEC monolayer in the lumen of the vascular constructs, a 100 µg/ml solution of Alexa-Fluor-488 labeled dextran (10 kDA) in PBS was passed through the lumen of the constructs. Fluorescent images were captured every 10 min for up to 60 min at the same location of the device. The fluorescent intensities were plotted using the plot profile function of ImageJ software along a straight line across the tube near half way from both ends. The data were obtained in triplicates with at least three scanning lines for each construct and repeating the measurements in three constructs for each set of results. The obtained fluorescent intensities were normalized by dividing with the maximum intensity value in the vessel which was the intensity along the center axis line. Finally, the barrier to the diffusion was calculated from the temporal change in relative intensity at a distance 300 µm from the center line at different time points.

## 3 Results and discussions

In this paper we present the development of a multi-layered blood vessel-like structures on a microfluidic platform. These fabricated blood vessel-like structures consisted of up to a tri-layered architecture with high reproducibly and consistency. Furthermore, the mechanical properties of each layer of the wall, the number of cell lines to be incorporated, the cell types

and the cell density in individual layers could each be independently tuned.

### 3.1 Fabrication of Tri-layered vascular structure using GelMA hydrogel in microfluidic device

The detailed step-by-step process for fabrication of the tri-layer vascular structure is shown in Fig. 1a. The perfusion of cell culture media through fabricated vascular structure using a syringe pump is shown in Fig. 1b while a schematic drawing of the three arterial/vein layers is shown in Fig. 1c. The readily fabricated hollow channel in the vessel allowed perfusion of media, as shown using a fluorescent dye in Figs. 2a (i) and (ii). In addition, cells can be encapsulated in GelMA hydrogel to form monolayered, Figs. 2b (i), (ii), and multilayered vascular walls Figs. 2c (i), (ii) and (iii)). The construction of multilayered wall structure is demonstrated using fluorescent microbeads of red, blue and green colors, Fig. 2c. Fabrication of vascular structures with different thicknesses and lumen diameters can be achieved by using combinations of different stainless steel needle pairs as shown in Table 1. For example, a pair of 27G BD needle (outer diameter: 400 µm, ID: 196 µm) with a 120 µm Serine needle inside the 1.2 mm glass capillary resulted in a vascular-like structure with an outer diameter: 1.2 mm, thickness of adventitia layer: 400 µm, thickness of tunica media layer: 140 µm and a lumen diameter of 120 µm, as shown in Fig. 2(c) (ii). Similarly, a pair of 21G and 27G BD needles resulted in a vessel with the outer diameter, adventitia thickness, media thickness and lumen diameter of 1.2 mm, 200 µm, 200 µm and 400 µm respectively.

In native cardiovascular systems, the outer and lumen diameter of the vessels, the thickness of different wall layers and the mechanical properties of the tissue matrix vary in different layers. For example, the vascular walls for vessels close to the heart are thicker compared to those of vessels far away. Similarly, the relative thickness of tunica media and adventitia vary between the elastic and muscular arteries. Thus, the ability to independently control the thickness of different layers along with the luminal and outer diameter, as described in this study, can be useful in the development of biomimetic blood vessels-like structures of different types. In addition, the composition and mechanical properties of different layers of physiological blood vessels also differ among themselves. While the ECM of tunica media is highly elastic, comprised of collagen type I and III, elastin and several proteoglycans, the ECM in adventitia are more collagen rich. Our method also allows variation of composition and mechanical properties of individual layers of the tri-layer constructs. By varying the concentration of GelMA, for example, or possibly by incorporating different bio-active compounds (peptides, proteins etc.) in the GelMA prepolymer solution, the mechanical properties and biological responses of different layers can be independently controlled.

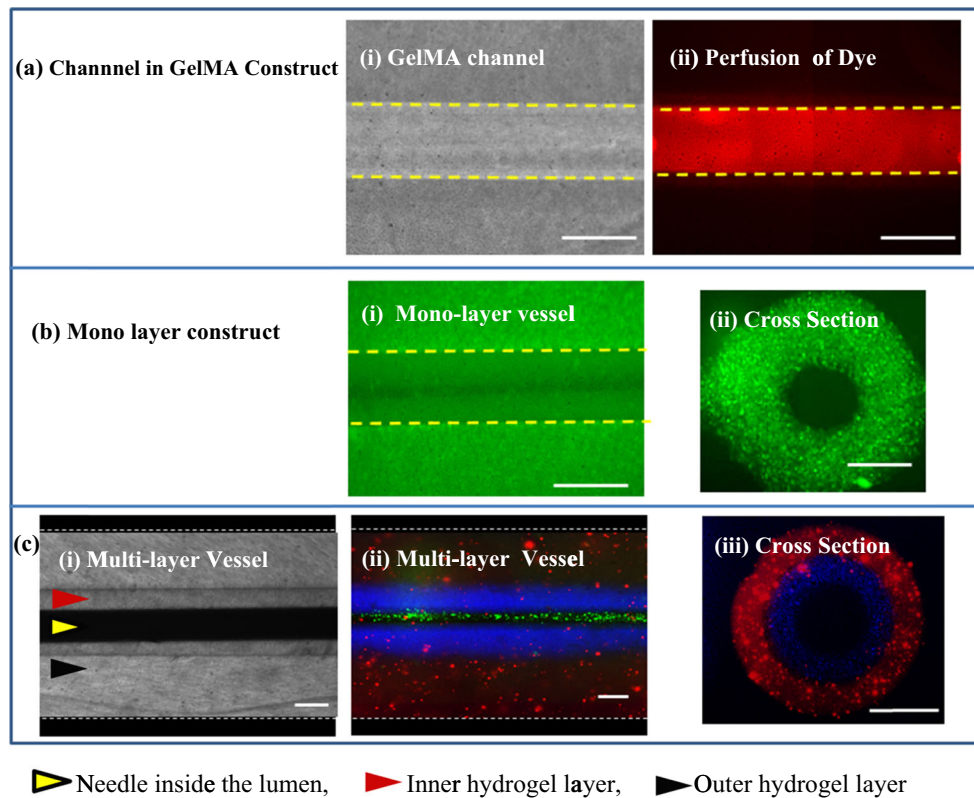


**Fig. 2** Illustration of the single and multilayer vascular-like structures, **a** a tubular Channel fabricated in bare GelMA: (i) phase contrast images of a 200  $\mu\text{m}$  channel in bare GelMA, (ii) fluorescent image after flowing FITC through a 200  $\mu\text{m}$  channel in GelMA; **b** a single layer vascular-like construct; (i) fluorescent image of top view of the vascular-like structure with green fluorescent beads encapsulated in the wall, (ii) cross-sectional

side view of the structure showing the lumen and the wall of the construct; **c** a multilayer vascular-like structure: (i) top view bright field image of the bilayer structure, (ii) top view of the bilayer structure with fluorescent beads of different colors encapsulated in different layers, (iii) cross-sectional side view of the structure showing the lumen and the two layers of the wall. Scale bars=200  $\mu\text{m}$

### 3.2 Effect of GelMA concentration on tube formation

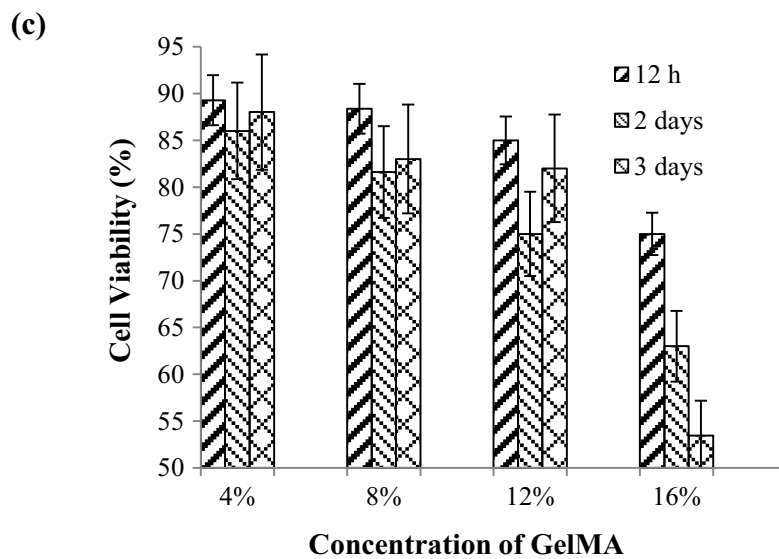
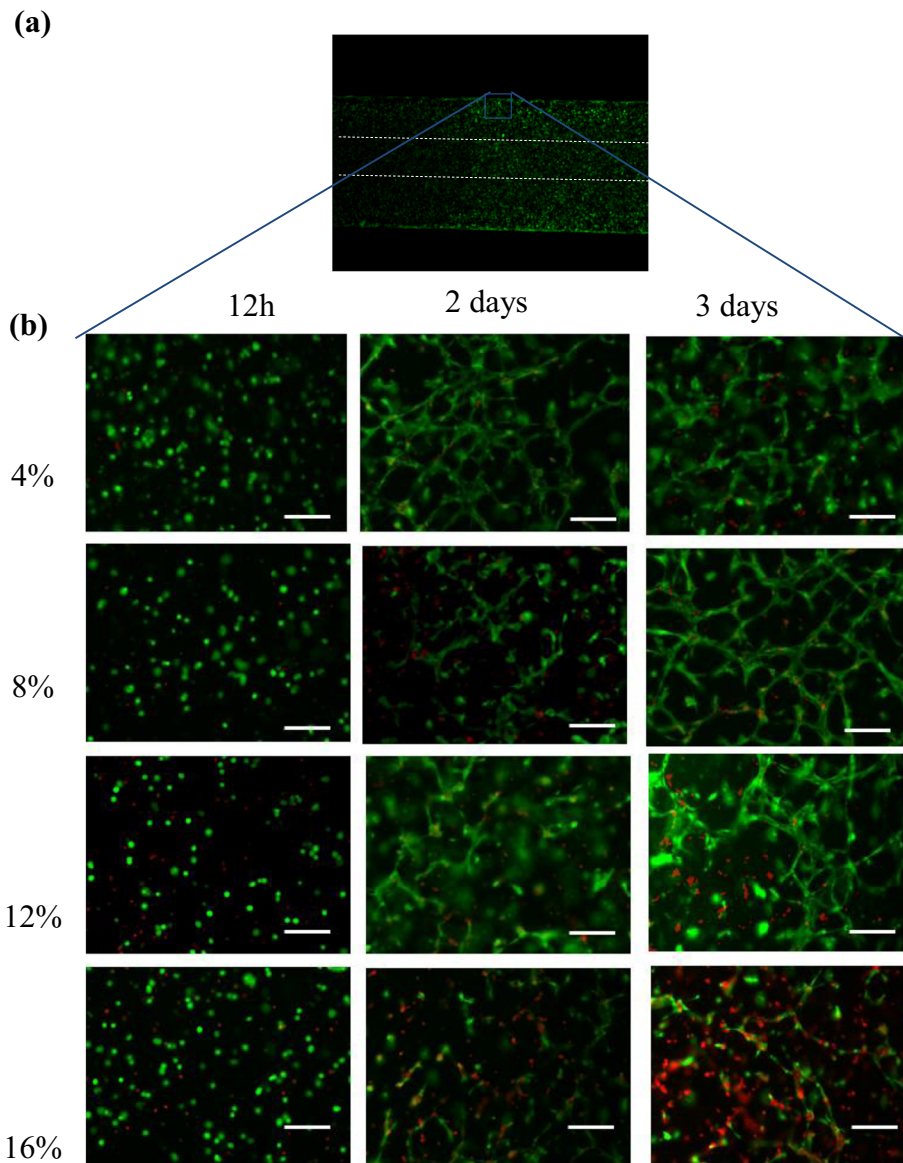
The method used in this study for fabrication of vascular-like structures is based on molding of photocrosslinkable GelMA hydrogel around stainless steel needles and smoothly removing the needles after the gel layers are formed. In order to facilitate the smooth retraction of needles from the gel, the needles were pre-coated with BSA by soaking them in a 1 % BSA solution for 40 min. However, it was noticed that

the concentration of GelMA played a more prominent role in determining how smoothly the needles could be removed from the gel. A set of representative images of tubes formed using different concentrations (e.g., 4, 8, and 12 %) of GelMA is shown in supplementary Figure, Fig. S1. It is evident that the tubes with mechanically weaker hydrogels (4 % GelMA) got severely damaged with clearly visible cracks, tears, and wavy undulations during the retrieval of needle. For gels of higher concentrations (12 % and

**Table 1** Specifications of the vascular-like constructs that can be fabricated using combinations of needle pairs of different sizes

Specifications of glass capillary and needles								Specifications of fabricated vascular constructs				
Capillary diameter (mm)	Outer needle			Inner needle			Adventitia ( $\mu\text{m}$ )	Media ( $\mu\text{m}$ )	Lumen ( $\mu\text{m}$ )	Vessel diameter (mm)	Total wall thickness	
	Gage	OD ( $\mu\text{m}$ )	ID ( $\mu\text{m}$ )	Gage	OD ( $\mu\text{m}$ )	ID ( $\mu\text{m}$ )						
1	1.2	27G	400	196	120S	120	N/A	400	140	120	1.2	540
2	1.2	25G	508	406	200S	200	N/A	346	164	200	1.2	500
3	1.2	21G	800	241	27G	400	196	200	200	400	1.2	200
4	0.6	27G	400	196	120S	120	N/A	100	102	120	0.6	240
5	1.2	25G	508	406	200S	200	N/A	42	154	200	0.6	200
6	6	18G	1000	Monolayer vessel for mechanical test				2500	-	1000	6.0	2500





◀ **Fig. 3** Viability of 3T3 fibroblast cells in the walls of the fabricated vascular structure of cell encapsulated GelMA at different concentrations over time. The cell-laden GelMA constructs were stained with Calcein-AM (green) and ethidium homodimer (red) at 12 h, 2 and 3 days after encapsulation, **a** a vascular construct showing the cells encapsulation in the vascular structure of GelMA, **b** live-dead staining of 4, 8, 12 and 16 % GelMA constructs after 12 h, 2 and 3 days, **c** cell viability at different time points in 4, 8, 12 and 16 % GelMA constructs after 12 h, 2 and 3 days. Cell viability in the low concentration GelMA constructs were considerably higher compared to high density GelMA. Scale bars=100  $\mu\text{m}$

higher) the luminal surface of the tubes after retrieval of needles were smooth and relatively defect-free. The higher concentration GelMA was therefore easier for fabrication of vessels from structural and mechanical perspectives. However, too high of a concentration is not helpful for good cell viability. Therefore obtaining optimum concentration is important.

While previous studies on collagen and fibrin hydrogel reported contraction of the vessel after EC seeding followed by expansion due to the forces from cells (Wong et al. 2010), the GelMA vessels, particularly those from higher GelMA concentrations, did not show any significant change in diameter after cell seeding. This could possibly be attributed to the higher stiffness i.e., the better mechanical properties of GelMA hydrogel compared to collagen and fibrin hydrogels. For low concentration GelMA, particularly the 4 % gels, the vessels did appear to contract after seeding of HUVECs, however, those concentrations were not used in subsequent experiments. Similarly, we did not observe any invasion of HUVECs from the lumen surface into the gel matrix.

### 3.3 Viability of cells in the walls of fabricated vessels

To understand the effect of GelMA concentration on the viability of encapsulated cells in the wall and to further tune the GelMA concentration for fabrication of vessels, the viability of fibroblast cells in the wall was investigated for different GelMA concentrations (4, 8, 12 and 16 %). In this attempt, the vascular structure after fabrication were taken out of the microfluidic device and cultured in multiwell plates inside an incubator. The live-dead images and the viability fibroblast cells in the walls of the fabricated vessels performed at different time points are shown in Figs. 3a–c. The 4–12 % concentration samples showed higher cell viability compared to 16 % concentration samples.

### 3.4 Effect of lumen diameter on seeding of HUVECs

While most tubes formed in this study had an initial lumen diameter of 200  $\mu\text{m}$ , we also formed the endothelial monolayer in tubes of four other sizes i.e., 120, 180, 300 and 400  $\mu\text{m}$ . These tubes were made using Seirin needles 120S, 180S,

300S, and BD needle 27G respectively. Some tubes of 120  $\mu\text{m}$  lumen-diameter occasionally became clogged during cell seeding and seized to flow when a high cell density were used in seeding. We used a lower cell density,  $15 \times 10^6$  cells/ml, for effective seeding of these small diameter tubes. In larger diameter tubes, i.e., 300 and 400  $\mu\text{m}$ , higher (up to  $30 \times 10^6$  cells/ml) cell densities were used.

The seeding was relatively difficult for larger diameter vessels as most cells entering from one end of the tube would pass through the tube and exit from the other end leaving very small number of cells retained inside the tube. It is known from physics of fluid flow that the flow resistance is inversely proportional to the square of the tube diameter.

### 3.5 Cell adhesion and HUVECs monolayer formation

Formation of a continuous monolayer of ECs in the luminal surface is essential for fabrication of a functional blood vessel mimic. Hence, the adhesion and spreading of ECs on the luminal surface must be ensured. We optimized the adhesion of HUVECs on 4, 8, 12, and 16 % micropatterned GelMA 2D surface. The adhesion and spreading of HUVECs on 2D GelMA surface at different time points are shown in Fig. 4a while the area of confluency as quantified using the image analysis software ImageJ is presented in Fig. 4b. The spreading of HUVECs in the GelMA channel over time is shown in Fig. 4c while Fig. 4d shows the actin-DAPI staining of a HUVEC monolayer inside the lumen of a vessel. The high concentration GelMA showed consistently higher adhesion and spreading of cells. For 16 % GelMA, by day 3 after seeding, an area of confluency of over 60 % was achieved while those for 4, 8, and 12 % GelMA were about 20, 30 and 45 % respectively, Figs. 4a and b. This trend is consistent with earlier reports (Nichol et al. 2010) where the area of confluency for 5 and 10 % GelMA with a cell seeding density of  $2 \times 10^6$  cells/ml were about 10 and 18 % respectively, i.e., the higher concentration of GelMA exhibited higher cell adhesion and spreading. The values for the area of confluency was consistently higher in the current study compared to earlier reported studies on GelMA, for example Nichol and coworkers (Nichol et al. 2010). This is because, the cell density used in this study was 5 million/ml as opposed to 2 million/ml in earlier ones (Nichol et al. 2010). It is also evident that higher GelMA concentrations help in faster spreading of surface seeded HUVECs, Fig. 4a. However, lower concentration of GelMA results in better viability for cells encapsulated in 3D, Fig. 3b and c. Hence, based on these findings for optimum combination of the two, we chose the 8 and 12 % GelMA concentrations for subsequent fabrications. The formation of a confluent monolayer of HUVECs, in the luminal surface of the fabricated vessel, is evident by day 3 from Fig. 4c, which is also confirmed by the staining of cytoskeletal Actin fibers using Alexa fluor 488 (green) and DAPI staining (blue) of cell nucleus as shown in

Fig. 4d. It is worth noting that even though the confluency of HUVECs on 2D surface seeded on 16 % GelMA on day 3 was about 60 %, as shown in Fig. 4a and b, the confluency on the luminal surface of the tube on day 3 was over 90 %. The higher confluency in the lumen of the tube can be attributed to the effect of shear flow in the lumen and the higher cell density i.e., 20 million/ml as opposed to 5 million/ml on 2D surface.

### 3.6 Mechanical properties

The successful application of tissue engineering requires that the mechanical properties of the engineered tissues be suitable for the specific *in vivo* application (Hasan et al. 2014c). We, therefore, investigated the uniaxial compressive mechanical properties of the fabricated vessels for GelMA concentrations of 4, 8, 12 and 16 % as described in section 2.9. The compressive stress–strain curves for up to 50 % strain are shown in supplementary Figure, Fig. S2 (a) while the compressive modulus, failure stress and failure strain at different concentrations of GelMA are shown in Figs. S2 (b), (c) and (d) respectively.

Fig. 5 Permeability of fluorescently labeled 10 kDa dextran to the walls of the vessel-like structures from the flow in the lumen: **a** a vessel without any EC layer at time zero of starting the dextran perfusion, **b** a vessel with an EC monolayer at time zero of starting perfusion, **c** a vessel without any EC layer after 20 min of dextran perfusion, **d** a vessel with an EC monolayer after 20 min of dextran perfusion. **e** and **f** Change in relative intensity of fluorescence with respect to the distance from the center of the vessels for the vascular-like structures without and with the EC monolayer respectively. The fluorescent intensity from line scanings across the vessels orthogonal to the axial direction at their center in **a** and **b** was measured at a time interval of 10 min. The intensities were then normalized against the maximum intensity values at the center of the vessel. **g** and **h** The relative intensity values at a distance 300  $\mu\text{m}$  from the center of the vessels at different time points. The barrier function was obtained from the slope of the relative intensity versus time graphs in **g** and **h**. Scale bars=200  $\mu\text{m}$

The higher concentration GelMA samples showed higher stiffness (modulus) and failure stress while the failure strains consistently decreased with increasing concentration. An increase of GelMA concentration from 4 to 16 % increased the compressive modulus by almost 44 times, to 138 kPa from 3.1 kPa, while the failure stress increased to 175 kPa from 43 kPa and

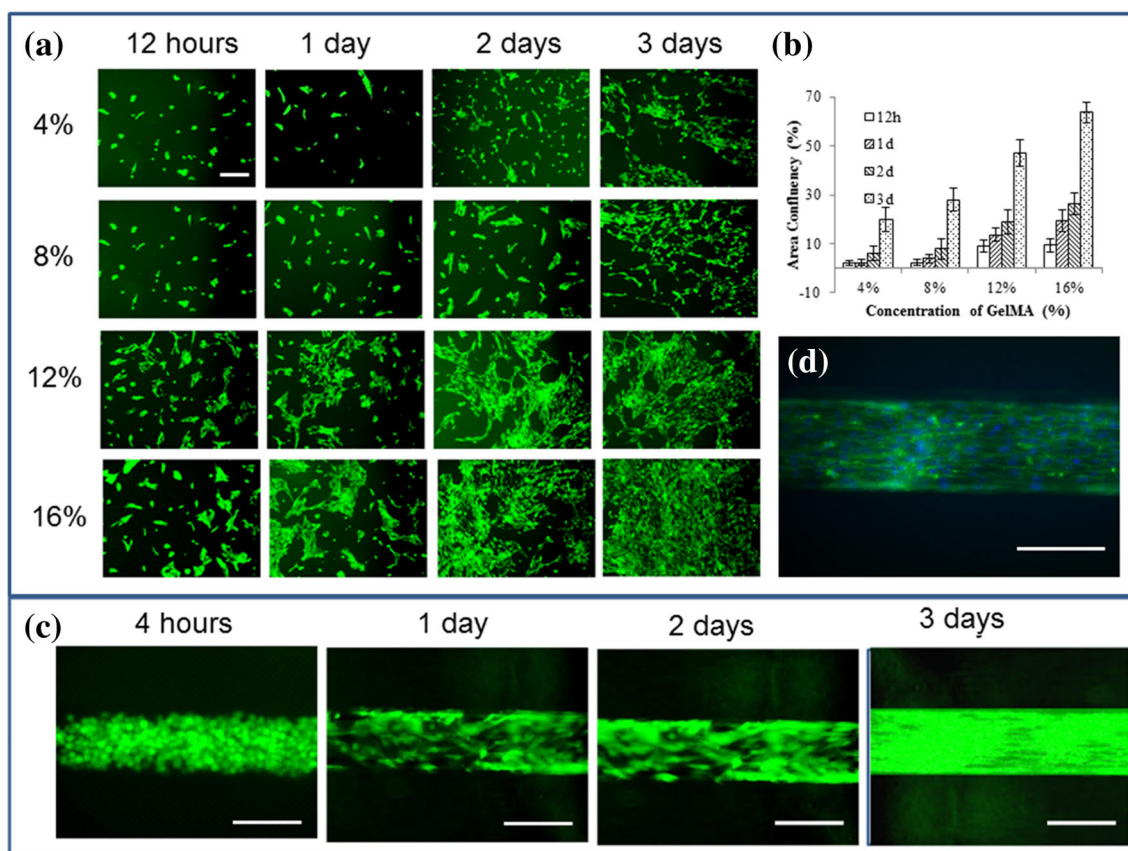
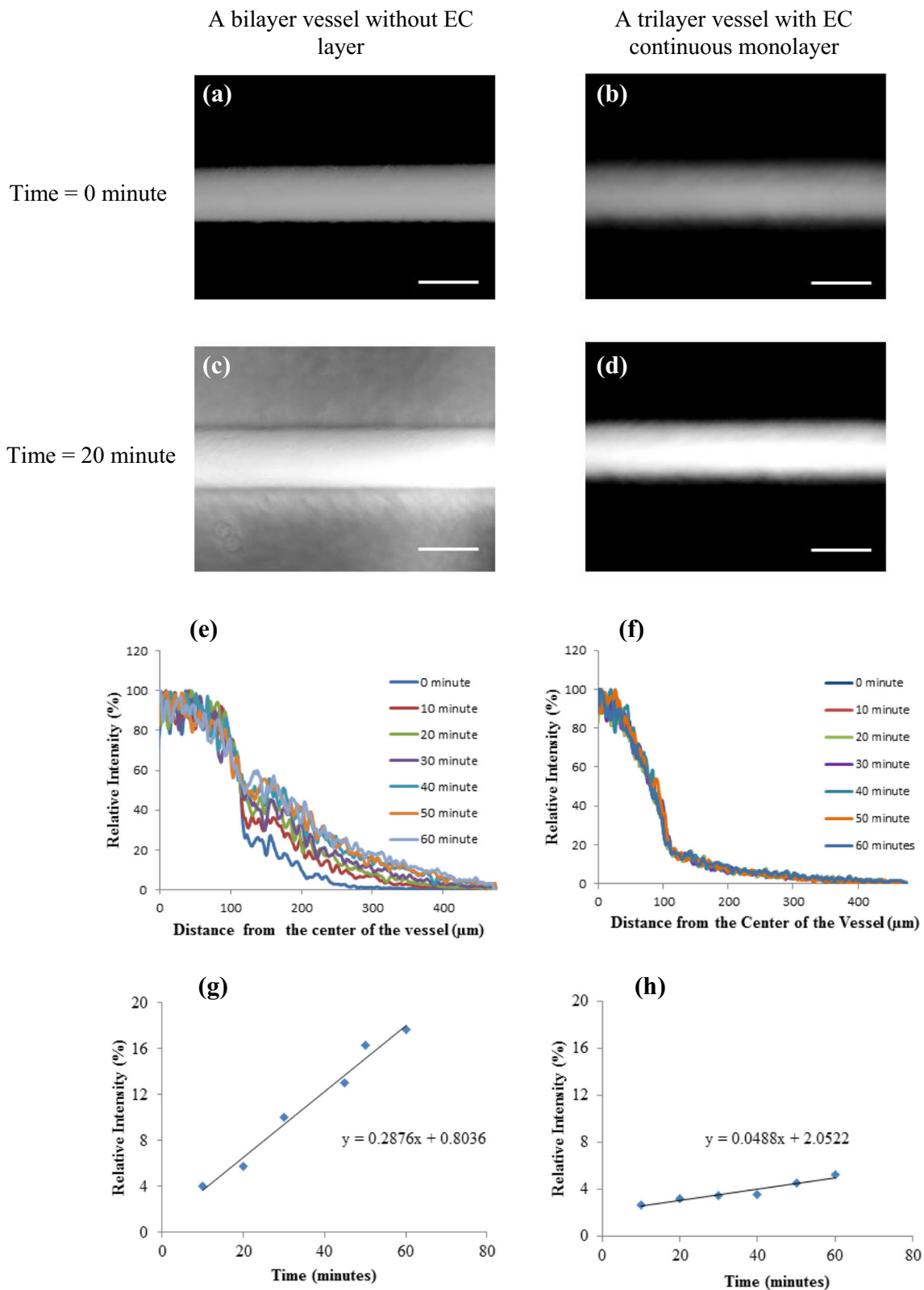


**Fig. 4** Formation of the EC monolayer on 2D GelMA surface and inside the lumen of the vascular-like structure, **a** GFP-fluorescent images showing attachment, spreading and growth of HUVECs on 2D GelMA surface at 4, 8, 12 and 16 % GelMA concentrations after 12 h, 1, 2 and 3 days of cell seeding, **b** area of confluence of HUVECs on 2D GelMA surface over time for different GelMA concentrations. **c** Spreading of HUVECs inside the lumen of a vascular-like structure with 12 %

GelMA concentration over time, and **d** a representative Phalloidin-DAPI staining image showing the continuous monolayer of HUVECs in the channel at 12 % GelMA concentration after 3 days of cell seeding. The cells spread well on both the 2D surface and the luminal surface, forming a cell monolayer, as is seen from the actin skeleton (green) and the nucleus of the cells (blue). Scale bars in figures **a** are 100  $\mu\text{m}$  while those in figures **b** and **c** are 200  $\mu\text{m}$



the failure strain decreased to 58 % from 85 %. These values are quite low compared to those of native vascular structures which are usually in the MPa ranges. Therefore, the hydrogel-based

structures presented here are not mechanically strong enough for use as implantable replacement blood vessels during vascular surgeries, however, they can be highly useful in *in vitro*



study of vascular mechanobiology and development of blood vessels on chip models for drug screening and development of *in vitro* models for cardiovascular diseases.

### 3.7 Barrier functions and permeability of the vascular constructs

One of the requirements for functional vascular constructs is a strong barrier function offered by the EC monolayer on the luminal surface. In order to evaluate the barrier function, permeability of Alexa-Fluor-488 labeled dextran ( $M_w \sim 10$  kDA) through the tri-layered vascular constructs was compared with that of a bilayer vascular construct without any EC monolayer. The fluorescently labeled dextran was perfused through the constructs, and the fluorescence intensity of the diffused dextran in the walls of the constructs was measured at 10 min intervals for 60 min. The intensity distributions were obtained by line-scanning the fluorescent images near the center of the tubes using the plot profile function in ImageJ software. The relative intensity was obtained by normalizing against the intensity at the center of the channel, which was also the maximum intensity value along the respective curves. Fig. 5a and b show the fluorescence image of two vascular constructs, one without any HUVECs monolayer, and the other with a HUVECs monolayer at time zero of perfusing the fluorescent dextran through the lumen. Fig. 5c and d show those images after 20 min of continuous perfusion. The relative intensity distribution from the center of the channel to the walls of vessels are shown in Fig. 5e and f while the relative intensity values at a distance 300  $\mu\text{m}$  from the center of the channel, i.e., 200  $\mu\text{m}$  from the luminal surface at different time points are plotted in Figs. 5g and h respectively. These figures show a high rate of diffusion of dextran in the vascular construct without EC monolayer compared to the tri-layered vascular construct with a HUVEC monolayer. While the relative intensity in the construct without the EC monolayer continuously increased with time, the tri-layered vascular-like construct showed very small increase in the relative intensity with time, indicating a strong barrier effect by the EC monolayer. The diffusion properties in the constructs were compared using the slopes of the best fitting curves. The slopes for the bilayer vascular-like structure without any EC layer and the tri-layered construct with a continuous EC monolayer were  $2.87 \times 10^{-3} \text{ min}^{-1}$  and  $4.88 \times 10^{-4} \text{ min}^{-1}$  respectively, indicating an order of magnitude decrease in the diffusion properties due to the presence of EC monolayer in the construct.

## 4 Conclusions

Perfusible tri-layered blood vessel-like structures on a microfluidic platform has been developed. The method used in this study allows fabrication of a range of vascular-like

structures, with varying wall thicknesses as well as different thicknesses of the different wall layers, and different lumen diameters. The vascular-like structures developed using our technique were grown for several days with the continuous perfusion of media through the lumen of the vessels. The cells remained viable under this condition. The mechanical properties of the vascular constructs changed significantly depending on the concentration of GelMA. The developed vessels with a continuous EC monolayer demonstrated strong barrier functions compared to bare tubes without any EC monolayer. The multilayer vessel will have multifaceted applications including development of *in vitro* models of various cardiovascular diseases such as atherosclerosis and hypertension, study of cancer metastasis, on chip human-tissue-model for screening of potential drug candidates. In the future *in vitro* investigations of cell mechanobiology such as effects of flow and mechanical stresses on ECs to SMCs interactions and signaling cascades will also be assessed.

**Acknowledgments** Anwarul Hasan acknowledges the startup grant and the URB (University Research Board) grant from American University of Beirut, Lebanon, and the CNRS (National Council for Scientific Research) grant, Lebanon. Ali Khademhosseini acknowledges funding from the National Science Foundation (EFRI-1240443), IMMODGEL (602694), and the National Institutes of Health (EB012597, AR057837, DE021468, HL099073, AI105024, AR063745). The authors acknowledge the assistance from Gi Seok Jeong in drawing/editing a part of Fig. 1, and scientific/technical discussions with Joe Tien from Boston University. Arghya Paul likes to acknowledge the Institutional Development Award (IDeA) from the National Institute of General Medical Sciences, National Institutes of Health (NIH), under Award Number P20GM103638-04. Adnan Memic and Ali Khademhosseini would like to thank the National Plan for Science, Technology and Innovation (MAARIFAH) by King Abdulaziz City for Science and Technology, Grant No. 12-MED3096-3 for their support and funding of this project.

## References

- Barthes, H., Özçelik, M., Hindié, A., Ndreu-Halili, A., Hasan, N.E., Vrana, Cell microenvironment engineering and monitoring for tissue engineering and regenerative medicine: the recent advances. *BioMed research international* 2014, p. 18. doi:10.1155/2014/921905
- Benton, C.A., Deforest, V., Vivekanandan, K.S., Anseth, Photocrosslinking of gelatin macromers to synthesize porous hydrogels that promote valvular interstitial cell function. *Tissue Eng. Part A* **15**, 3221–30 (2009)
- Browning, D., Dempsey, V., Guiza, S., Becerra, J., Rivera, B., Russell, M., Höök, F., Clubb, M., Miller, T., Fossum, J.F., Dong, A.L., Bergeron, M., Hahn, E., Cosgriff-Hernandez, Multilayer vascular grafts based on collagen-mimetic proteins. *Acta Biomater.* **8**, 1010–21 (2012)
- Cao, P.R., Arany, Y.S., Wang, D.J., Mooney, Promoting angiogenesis via manipulation of VEGF responsiveness with notch signaling. *Biomaterials* **30**, 4085–93 (2009)
- Chen, E.A., Silva, W.W., Yuen, A.A., Brock, C., Fischbach, A.S., Lin, R.E., Guldberg, D.J., Mooney, Integrated approach to designing growth factor delivery systems. *Faseb J.* **21**, 3896–903 (2007)
- Chen, R.-Z., Lin, H., Qi, Y., Yang, H., Bae, J.M., Melero-Martin, A., Khademhosseini, Functional human vascular network generated in



- photocrosslinkable gelatin methacrylate hydrogels. *Adv. Funct. Mater.* **22**, 2027–39 (2012)
- K.M. Chrobak, D.R. Potter, J. Tien, Formation of perfused, functional microvascular tubes *in vitro*. *Microvasc. Res.* **71**, 185–96 (2006)
- S. Chung, R. Sudo, P.J. Mack, C.-R. Wan, V. Vickerman, R.D. Kamm, Cell migration into scaffolds under co-culture conditions in a microfluidic platform. *Lab Chip* **9**, 269–75 (2009)
- D.C. Darland, P.A. D'Amore, TGF beta is required for the formation of capillary-like structures in three-dimensional cocultures of 10 T1/2 and endothelial cells. *Angiogenesis* **4**, 11–20 (2001)
- Y. Du, D. Crokep, M.R.K. Mofrad, E.J. Weinberg, A. Khademhosseini, J. Borenstein, in *Microfluidics for biological applications*, ed. by W.-C. Tian, E. Finehout (Springer, New York, 2008)
- A. Hasan, A. Memic, N. Annabi, M. Hossain, A. Paul, M.R. Dokmeci, F. Dehghani, A. Khademhosseini, Electrospun scaffolds for tissue engineering of vascular grafts. *Acta Biomater.* **10**, 11–25 (2014a)
- A. Hasan, A. Paul, N.E. Vrana, X. Zhao, A. Memic, Y.-S. Hwang, M.R. Dokmeci, A. Khademhosseini, Microfluidic techniques for development of 3D vascularized tissue. *Biomaterials* **35**, 7308–25 (2014b)
- A. Hasan, K. Ragaert, W. Swieszkowski, S. Selimović, A. Paul, G. Camci-Unal, M.R.K. Mofrad, A. Khademhosseini, Biomechanical properties of native and tissue engineered heart valve constructs. *J. Biomech.* **47**, 1949–63 (2014c)
- A. Hasan, M. Nurunnabi, M. Morshed, A. Paul, A. Polini, T. Kuila, M. Al Hariiri, Y.-k. Lee, A.A. Jaffa, Recent advances in application of biosensors in tissue engineering. *BioMed research international* 2014, p. 18 (2014d)
- A. Hasan, A. Khattab, M.A. Islam, K.A. Hweij, J. Zeitouny, R. Waters, M. Sayegh, M. Hossain, A. Paul, Injectable hydrogels for cardiac tissue repair after myocardial infarction. *Adv. Sci.* (2015). doi:10.1002/advs.201500122
- T. Kaully, K. Kaufman-Francis, A. Lesman, S. Levenberg, Vascularization - the conduit to viable engineered tissues. *Tissue Eng. Part B Rev.* **15**, 159–69 (2009)
- A. Khademhosseini, J. Yeh, G. Eng, J. Karp, H. Kaji, J. Borenstein, O.C. Farokhzad, R. Langer, Cell docking inside microwells within reversibly sealed microfluidic channels for fabricating multiphenotype cell arrays. *Lab Chip* **5**, 1380–6 (2005)
- A. Khademhosseini, J. Yeh, S. Jon, G. Eng, K.Y. Suh, J.A. Burdick, R. Langer, Molded polyethylene glycol microstructures for capturing cells within microfluidic channels. *Lab Chip* **4**, 425–30 (2004)
- J.E. Leslie-Barbick, J.J. Moon, J.L. West, Covalently-immobilized vascular endothelial growth factor promotes endothelial cell tubulogenesis in poly(ethylene glycol) diacrylate hydrogels. *J. Biomater. Sci. Polym. Ed.* **20**, 1763–79 (2009)
- J.E. Leslie-Barbick, J.E. Saik, D.J. Gould, M.E. Dickinson, J.L. West, The promotion of microvasculature formation in poly(ethylene glycol) diacrylate hydrogels by an immobilized VEGF-mimetic peptide. *Biomaterials* **32**, 5782–9 (2011a)
- J.E. Leslie-Barbick, C. Shen, C. Chen, J.L. West, Micron-scale spatially patterned, covalently immobilized vascular endothelial growth factor on hydrogels accelerates endothelial tubulogenesis and increases cellular angiogenic responses. *Tissue Eng. Part A* **17**, 221–9 (2011b)
- L.F. Mendes, R.P. Pirraco, W. Szymczyk, A.M. Frias, T.C. Santos, R.L. Reis, A.P. Marques, Perivascular-like cells contribute to the stability of the vascular network of osteogenic tissue formed from cell sheet-based constructs. *PLoS One* **7**, e41051 (2012)
- J.S. Miller, K.R. Stevens, M.T. Yang, B.M. Baker, D.H.T. Nguyen, D.M. Cohen, E. Toro, A.A. Chen, P.A. Galie, X. Yu, R. Chaturvedi, S.N. Bhatia, C.S. Chen, Rapid casting of patterned vascular networks for perfusable engineered three-dimensional tissues. *Nat. Mater.* **11**, 768–74 (2012)
- M.N. Nakatsu, R.C.A. Sainson, J.N. Aoto, K.L. Taylor, M. Aitkenhead, S. Pérez-del-Pulgar, P.M. Carpenter, C.C.W. Hughes, Angiogenic sprouting and capillary lumen formation modeled by human umbilical vein endothelial cells (HUVEC) in fibrin gels: the role of fibroblasts and Angiopoietin-1. *Microvasc. Res.* **66**, 102–12 (2003)
- J.W. Nichol, S.T. Koshy, H. Bae, C.M. Hwang, S. Yamanlar, A. Khademhosseini, Cell-laden microengineered gelatin methacrylate hydrogels. *Biomaterials* **31**, 5536–44 (2010)
- E.C. Novosel, C. Kleinhans, P.J. Kluger, Vascularization is the key challenge in tissue engineering. *Adv. Drug Deliv. Rev.* **63**, 300–11 (2011)
- A. Paul, A. Hasan, H.A. Kindi, A.K. Gaharwar, V.T.S. Rao, M. Nikkhah, S.R. Shin, D. Krafft, M.R. Dokmeci, D. Shum-Tim, A. Khademhosseini, Injectable graphene oxide/hydrogel-based angiogenic gene delivery system for vasculogenesis and cardiac repair. *ACS Nano* **8**, 8050–62 (2014)
- G.M. Price, K.H.K. Wong, J.G. Truslow, A.D. Leung, C. Acharya, J. Tien, Effect of mechanical factors on the function of engineered human blood microvessels in microfluidic collagen gels. *Biomaterials* **31**, 6182–9 (2010)
- A. Ratcliffe, Tissue engineering of vascular grafts. *Matrix Biol.* **19**, 353–7 (2000)
- N. Sadr, M. Zhu, T. Osaki, T. Kakegawa, Y. Yang, M. Moretti, J. Fukuda, A. Khademhosseini, SAM-based cell transfer to photopatterned hydrogels for microengineering vascular-like structures. *Biomaterials* **32**, 7479–90 (2011)
- J.E. Saik, M.K. McHale, J.L. West, Biofunctional materials for directing vascular development. *Curr. Vasc. Pharmacol.* **10**, 331–41 (2012)
- A. Shamloo, S.C. Heilshorn, Matrix density mediates polarization and lumen formation of endothelial sprouts in VEGF gradients. *Lab Chip - Miniaturisation Chem. Biol.* **10**, 3061–8 (2010)
- A. Shamloo, H. Xu, S. Heilshorn, Mechanisms of vascular endothelial growth factor-induced pathfinding by endothelial sprouts in biomaterials. *Tissue Eng. Part A* **18**, 320–30 (2012)
- R. Sudo, S. Chung, I.K. Zervantonakis, V. Vickerman, Y. Toshimitsu, L.G. Griffith, R.D. Kamm, Transport-mediated angiogenesis in 3D epithelial coculture. *Faseb. J.* **23**, 2155–64 (2009)
- J.V. Tu, C.L. Pashos, C.D. Naylor, E. Chen, S.-L. Normand, J.P. Newhouse, B.J. McNeil, Use of cardiac procedures and outcomes in elderly patients with myocardial infarction in the united states and Canada. *N. Engl. J. Med.* **336**, 1500–5 (1997)
- A.I. Van Den Bulcke, B. Bogdanov, N. De Rooze, E.H. Schacht, M. Cornelissen, H. Berghmans, Structural and rheological properties of methacrylamide modified gelatin hydrogels. *Biomacromolecules* **1**, 31–8 (2000)
- K.H.K. Wong, J.G. Truslow, J. Tien, The role of cyclic AMP in normalizing the function of engineered human blood microvessels in microfluidic collagen gels. *Biomaterials* **31**, 4706–14 (2010)
- J.H. Yeon, H.R. Ryu, M. Chung, Q.P. Hu, N.L. Jeon, *In vitro* formation and characterization of a perfusable three-dimensional tubular capillary network in microfluidic devices. *Lab Chip* **12**, 2815–22 (2012)
- H. Yoshida, M. Matsusaki, M. Akashi, Multilayered blood capillary analogs in biodegradable hydrogels for *in vitro* drug permeability assays. *Adv. Funct. Mater.* **23**, 1736–42 (2012)
- W.W. Yuen, N.R. Du, C.H. Chan, E.A. Silva, D.J. Mooney, Mimicking nature by codelivery of stimulant and inhibitor to create temporally stable and spatially restricted angiogenic zones. *Proc. Natl. Acad. Sci. U. S. A.* **107**, 17933–8 (2010)
- Y. Zheng, J. Chen, M. Craven, N.W. Choi, S. Totorica, A. Diaz-Santana, P. Kermani, B. Hempstead, C. Fischbach-Teschl, J.A. López, A.D. Stroock, *In vitro* microvessels for the study of angiogenesis and thrombosis. *Proc. Natl. Acad. Sci. U. S. A.* **109**, 9342–7 (2012)